



## Photosynthetic characteristics of upland cotton (*Gossypium hirsutum*) recessive genic male sterile line YA-1 with virescent trait

N. YANG\*, X.X. LIU\*, X.P. ZHANG\*\*, H.Q. DENG\*\*\*, X.L. SHEN#, and C.M. TANG\*+,

State Key Laboratory of Crop Genetics and Germplasm Enhancement, College of Agronomy,

Nanjing Agricultural University, 210095 Nanjing, China\*

Hunan Institute of Cotton Science, 410326 Changde, China\*\*

Taicang Cotton Breeding Center, 215488 Suzhou, China\*\*\*

Jiangsu Academy of Agricultural Sciences, 210000 Nanjing, China#

### Abstract

The upland cotton strain YA-1 can be used for hybrid seed production and recurrent selection. However, the effect of YA-1 virescent phenotype on photosynthetic traits remains unclear. This study demonstrated that the chlorophyll and carotenoid contents, light-saturation point, light-compensation point, and PSII reaction center activities are lower than those of green leaves of wide type. In contrast, light-energy utilization efficiencies, net photosynthetic rate, transpiration rate, stomatal conductance, concentrations of Rubisco and phosphoenolpyruvate carboxylase, photosynthetic performance indices, and energy distribution parameters of the yellowish leaves of YA-1 are higher than those of wild type green leaves. The lower expression of *GhHemL*, *GhSGRL*, and *GhCAO* genes impairs chlorophyll biosynthesis, while the downregulation of *GhZEP* and *GhNCED* disrupts carotenoid biosynthesis, altering the pigment composition in yellowish leaves. The yellowish phenotype of YA-1 had significant positive effects on photosynthetic efficiency. This finding provides a valuable basis for optimizing the use of YA-1 in cotton breeding programs.

**Keywords:** heterosis; male sterility; photosynthesis; upland cotton; virescent mutant.

### Introduction

More than 30 virescent mutants with yellowish leaves have been found in tetraploid cotton, and 26 related virescent mutants have been successfully identified (Song *et al.* 2012). After upland cotton (*Gossypium hirsutum*)

virescent lines controlled by recessive genes were crossed with conventional varieties, F1 showed obvious heterosis in yield and fiber quality (Zhou *et al.* 2021). Most virescent lines are controlled by recessive genes. True and false hybrids (with virescent lines as the female parent and green-leaved plants as the male parent) can be identified

### Highlights

- The photosynthetic rate of YA-1 yellow leaves is higher than wide-type green leaves
- The decrease in Chl *a/b* leads to a transformation of YA-1 from yellow to green
- YA-1 can serve as a distinct marker in breeding programs without compromising photosynthetic efficiency

Received 13 February 2025

Accepted 30 May 2025

Published online 16 July 2025

\*Corresponding author

e-mail: tangcm@njau.edu.cn

**Abbreviations:**  $C_i$  – intercellular CO<sub>2</sub> concentration;  $E$  – transpiration rate;  $F_0$  – original fluorescence;  $F_v/F_m$  – maximal photochemical efficiency;  $g_s$  – stomatal conductance;  $I$  – photosynthetically active radiation;  $I_c$  – light-compensation point;  $I_m$  – light-saturation point; PEPCase – phosphoenolpyruvate carboxylase;  $PI_{abs}$  – performance index of absorption;  $P_N$  – net photosynthetic rate;  $P_{Nmax}$  – light-saturated net photosynthetic rate;  $R_D$  – dark respiration rate; RH – relative humidity;  $T_{air}$  – air temperature.

**Acknowledgments:** This study was financially supported by the Key Laboratory of Cotton and Rapeseed (Nanjing) and grants from Postgraduate Research & Practice Innovation Program of Jiangsu Province (KYCX21\_0603).

**Availability of data and materials:** All data generated or analysed during this study are included in this published article [and its supplementary information files]. RNA sequencing data is stored in the GEO database (GEO accession number: GSE263515): <https://www.ncbi.nlm.nih.gov/geo/query/acc.cgi?acc=GSE263515>.

**Conflict of interest:** The authors declare that they have no conflict of interest.

by the yellowish color of their leaves, which enables the utilization of heterosis in upland cotton (Mao *et al.* 2019, Zhang *et al.* 2020).

Compared with green leaves, yellowish leaves are significantly different in pigment content, chloroplast structure, photosynthesis, and so on. The virescent character of upland cotton is related to lower chlorophyll and carotenoid contents (Song *et al.* 2011). The chloroplast development of virescent etiolated leaves is defective and thylakoid development is abnormal, but it is not different from that of the wild type after leaf development is complete (Li *et al.* 2018). The differentially expressed genes between the penultimate leaf of 58vsp and the wild type were mainly involved in the ribosome, photosynthesis, chlorophyll synthesis, and other pathways (Li *et al.* 2018). The maximum quantum yield of primary photochemistry ( $F_v/F_m$ ) and quantum yield of PSII ( $\Phi_{PSII}$ ) varied greatly among virescent mutants (Song *et al.* 2014). The difference in net photosynthetic rate between upland cotton virescent mutants and their wild types was not clear. Etiolation mutations are usually caused by genetic mutations related to pigment synthesis or decomposition. A single nucleotide mutation in the gene *Gachlh*, which controls chlorophyll synthesis, leads to the failure of chlorophyll synthesis and results in a yellowish leaf phenotype in *Gossypium arboreum* (Fan *et al.* 2023). Silencing of *GhPUR4* leads to yellowing leaves, a decrease in chlorophyll content, and abnormal chloroplast development; *GhPUR4* participates in early chloroplast development and chlorophyll biosynthesis (Mao *et al.* 2019). The silencing of *Chll*, *ChlD*, and *ChlH* turns normal green leaves into yellowish leaves, which indicates that the lower transcription level of any of the three genes may lead to a decrease in chlorophyll content and leaf color difference (Mao *et al.* 2018). These results indicate that the yellowish leaves affect chlorophyll synthesis, and may affect photosynthesis (Mao *et al.* 2018, Fan *et al.* 2023). Therefore, elucidating the photosynthetic characteristics and genetic basis of virescent mutants has important theoretical and application value. Virescent lines can be utilized as a reliable marker for cotton hybrid production if yellowish leaves do not have a significant negative effect on photosynthesis.

There is F1 heterosis between different upland cotton varieties, and male sterile lines are of great significance for hybrid seed production (Mao *et al.* 2018). In the process of large-scale hybrid seed production using a male sterile line controlled by one recessive nuclear gene, 50% of the plants exhibit male sterility and serve as the female parent. Concurrently, the 50% of male fertile plants must be eliminated. The key problem is that there are false hybrids in F1 that cannot be found and removed in seedlings due to the unclean extraction of male fertile plants. YA-1 is a genic male sterile upland cotton line with recessive virescent trait. The young leaves of YA-1 are yellowish and turn green gradually with the growth of leaves, the yellowish leaves and male sterility are controlled by two different recessive nuclear genes. The male sterile plant (msms) of YA-1 is crossed with the fertile plant (Msms), and the ratio of male sterile plants to fertile plants in the next generation is 1:1 (msms:Msms). The population

can be used as a female parent in the production of hybrid seeds (F1). The male fertile plants were removed, and the male sterile plants with yellowish leaves controlled by recessive gene were used as the female parents. The restorer lines with green leaves controlled by the dominant gene were used as the male parents for hybrid seed production. The plants with yellowish leaves in F1 hybrids were pseudo-hybrid and the plants with green leaves were true hybrid. The purity of hybrids can be tested and false hybrid plants with yellowish leaves can be removed at the seedling stage. The F1 between YA-1 and upland cotton cultivars can be used in cotton production. However, it is not clear whether the virescent character of YA-1 affects its photosynthetic ability. The purpose of this study is to analyze the difference in pigment content, photosynthetic characteristics, and related gene expression between yellowish leaves of YA-1 and green leaves of wide type. The results will provide a basis for the application of YA-1 genic male sterile strain in upland cotton breeding.

## Materials and methods

**Plant materials:** Virescent mutant line V-1 controlled by recessive vv genotype was selected from upland cotton cultivar Sumian 12 irradiated by Co<sup>60</sup>. V-1 was crossed with male sterility line A1 (msms), F1 plants were self-crossed, and the plants with virescent and male fertility in F2 were crossed with male sterility plants of A1. The male fertility plants (VvMsms) were self-crossed after four backcross generations. The plants with virescent (YA-1) and green leaves (wild type, WT) in the next generation were selected to test in all experiments.

The indoor experiments were planted in a nutrient substrate (nutrient soil: vermiculite = 1:1), exposed to 16 h light (28°C)/8 h dark (25°C), relative humidity of 70%. For the outdoor experiment, plants were cultivated in a nutrient substrate (nutrient soil: vermiculite = 1:1), light at 25–32°C/dark at 18–25°C, daily average light exposure  $\geq 8$  h, and relative humidity of 65–75%. YA-1 shows yellowish leaves when the first true leaf unfolds. The etiolated leaf gradually turned green with the growth and development of the leaves. When the fourth true leaf unfolds, the color of the first yellowish leaf is similar to the WT green leaf. The apical new leaves of YA-1 plants showed yellowish during the whole growth period, and then gradually turned green similar to WT leaf color during growth (Fig. 1S, *supplement*).

**The difference in pigment composition in yellowish and green leaves of YA-1:** Three first fully unfolded YA-1 yellowish true leaves and three WT green leaves were randomly selected. The leaves were cut into fine filaments, 200 mg was accurately weighed, and extracted with 10 mL of 80% acetone in the dark until the leaves were whitened or transparent. The leaf pigment extract in 80% acetone was scanned by spectrophotometer (*SpectraMax iD5*, USA) in the wavelength range of 340–1,000 nm and the control was 80% acetone. The OD value was determined every 10 nm, and the spectral scanning map of the pigment extract was drawn.

**Chlorophyll (Chl) content in leaves:** Five leaves of YA-1 and WT at different growth stages were randomly selected, and the leaves were cut into 2-mm filaments, mixed and weighed to reach 200 mg, and then extracted with 10 mL of 80% acetone until the leaves became white or transparent. With 80% acetone as a control, the OD values of YA-1 and WT samples were determined at 663, 646, and 470 nm. The contents of total chlorophyll (total Chl), chlorophyll *a* (Chl *a*), chlorophyll *b* (Chl *b*), and carotenoid in leaves were calculated according to the method of Wang and Huang (2015).

**Net photosynthetic rate:** The photosynthetic parameters of YA-1 yellowish leaves and WT green leaves at different growth stages (two real leaf stages and bud stages) were tested with *LI-6400* (*LI-COR, Inc.*, Lincoln, Nebraska, USA) on a sunny morning. The parameters included net photosynthetic rate ( $P_N$ ), stomatal conductance ( $g_s$ ), intercellular carbon dioxide concentration ( $C_i$ ), and transpiration rate ( $E$ ). The *6400-02* LED light source of the system was used. The light intensity was set to  $1,000 \mu\text{mol}(\text{photon}) \text{m}^{-2} \text{s}^{-1}$ , and the gas flow was set to  $500 \mu\text{mol} \text{s}^{-1}$ . Measurements were set at a seedling stage temperature of  $27.4^\circ\text{C}$ , a relative humidity of 70.2%, and a vapor pressure deficit of 1.16 kPa. For the bud stage, conditions included a temperature of  $32.6^\circ\text{C}$ , the same relative humidity of 70.2%, and a vapor pressure deficit of 1.47 kPa. The temperature and humidity of the leaf chamber were consistent with the atmosphere.

**Diurnal variation in photosynthetic rate:** Four penultimate leaves of the main stem of YA-1 yellowish leaves and four WT green leaves were selected, and the net photosynthetic rate was measured every hour from 9:00 to 17:00 h in sunny weather. Each determination was completed within 30 min. The *6400-02* LED light source of the system was used in the measurement, the light intensity was set to the natural light intensity, the gas flow rate was set to  $500 \mu\text{mol} \text{s}^{-1}$ .

**Light-response curve:** On a sunny morning, the light-response curves of the photosynthetic rate of four typical YA-1 yellowish leaves and four green leaves of wild type were measured with *LI-6400* (*LI-COR, Inc.*, Lincoln, Nebraska, USA). The light intensity was set to 2,000; 1,500; 1,000; 500; 300; 200; 150; 100; 50, and  $0 \mu\text{mol}(\text{photon}) \text{m}^{-2} \text{s}^{-1}$ . During the measurement, the *6400-02 LED* light source of the system was used, the gas flow rate was set to  $500 \mu\text{mol} \text{s}^{-1}$ , and the temperature and humidity of the leaf room were consistent with the atmosphere. The automatic matching program was entered when the relative error of instrument measurement reached more than 5%. Light-saturated net photosynthetic rate ( $P_{N\text{max}}$ ), dark respiration rate ( $R_D$ ), light-saturation point ( $I_m$ ) and the light-compensation point ( $I_c$ ) used for the light-response model of photosynthesis (Ye *et al.* 2019):

$$P_N = \alpha \frac{1 - \beta I}{1 + \gamma I} I - R_D$$

$I$  is the photosynthetically active radiation,  $\alpha$ ,  $\beta$ , and  $\gamma$  are three parameters independent of light intensity.  $\alpha$  is

the initial slope of the light-response curve (dimensionless),  $\beta$  and  $\gamma$  are coefficients.  $P_N$  is the net photosynthetic rate.

**Phosphoenolpyruvate carboxylase (PEPCase) and ribulose-1,5-bisphosphate carboxylase (Rubisco) concentration:** The concentrations of PEPCase and Rubisco were quantitatively determined using a double-antibody sandwich enzyme-linked immunosorbent assay (ELISA). This method was applied to analyze samples from YA-1 and WT young and mature leaves under identical conditions. The standard concentrations (six standard wells plus one zero-concentration well, resulting in seven concentration points) were plotted on the horizontal axis. In contrast, the corresponding absorbance values ( $OD_{450}$ ) were plotted on the vertical axis. *ELISACalc* software was employed to fit a four-parameter logistic (4-PL) curve and generate a standard curve equation. The sample concentrations were calculated by inputting the  $OD_{450}$  values into the standard curve equation.

**Chl fluorescence parameters:** The five YA-1 yellowish leaves and WT green leaves were monitored at the same leaf position at different growth stages. After dark treatment (1 h), the Chl fluorescence parameters of leaves were measured by *Handy PEA* (*Hansatech, UK*). The probe and the dark-adaptation clip were pressed tightly, the metal light shielding film was opened, and the measurement function key was pressed to perform the measurement. After the measurement was completed, *PEA Plus V1.10* software was used to calculate the parameters, and 18 Chl fluorescence parameters were measured (Table 1S, *supplement*).

**RNA sequencing (RNA-seq) of YA-1 yellowish leaves and WT green leaves:** The RNA sequencing materials were the first spreading real yellowish leaf of YA-1 and green leaves of WT, three biological replicates were performed, with a total of 6 samples. A polysaccharides and polyphenols RNA extraction kit (*Tiangen, Beijing*) was used to extract RNA from leaves. Electrophoresis was performed, and a *One Drop (1000+)* spectrophotometer was used to detect the concentration and quality of RNA. The construction of the DNA library and sequencing were performed by the *Beijing Genomics Institute (BGI, Beijing)*. Data filtering was performed using *SOAPnuke* software (*BGI, Beijing*). Clean reads were obtained by removing the reads containing adapters, reads with more than 5% N, and low-quality sequences. The clean reads were spliced and aligned to the reference *G. hirsutum* genome retrieved from the cotton genome website (<https://www.cottongen.org/>). The fragments per kilobase per transcript per million mapped reads (FPKM) values were calculated and used to estimate the effects of sequencing depth and gene length on the mapped read counts.

**Screening and analysis of differentially expressed genes (DEGs):** The *DEG-seq R* package (*1.20.0*) was used to analyze DEGs with a corrected  $P$  value  $< 0.001$  and an absolute  $\log_2$  ratio  $\geq 1$ . *GO* (*Gene Ontology*) terms and *KEGG* (*Kyoto Encyclopedia of Genes and Genomes*)

pathways were enriched by DEGs if the  $P$  values were  $<0.001$ .

**Quantitative reverse-transcription-PCR (qRT-PCR) analysis:** The first fully unfolded yellowish true leaf of YA-1 and WT green leaves were verified by qRT-PCR, and 15 DEGs were randomly selected for verification. Data were collected from three replicate experiments, and the samples used for qRT-PCR were the same as those used for RNA-seq. RNA was extracted from sample leaves and reverse transcribed into cDNA. qRT-PCR was performed via a *Bio-Rad CFX96 Real-Time System* (*Bio-Rad*, USA), and each PCR mixture (20  $\mu\text{L}$ ) consisted of 10  $\mu\text{L}$  *SuperReal PreMix Plus SYBR Green* (*Tolbio*), 0.4  $\mu\text{L}$  of each primer, 2  $\mu\text{L}$  of cDNA, and 7.2  $\mu\text{L}$  of sterile water. Each sample involved at least three technical repeats. The PCR cycle included an initial denaturation step at 95°C for 10 min, followed by 40 cycles at 90°C for 30 s, 60°C for 30 s, and 72°C for 30 s. The upland cotton ubiquitin gene was used as an internal reference gene, and the expression of related genes was calculated by the  $2^{-\Delta\Delta C_t}$  method. The primers referenced the upland cotton gene fluorescence quantitative specific primer database *qPrimerDB* (<http://biodb.swu.edu.cn/qprimerdb/>) (Table 2S, *supplement*).

**Statistical analysis:** Data analysis and plotting were performed using *Excel XP*, *Origin 2024*, and *GraphPad Prism 10.1.2* software. *GraphPad Prism 10.1.2* was used to calculate the correlations between photosynthesis-related parameters and Chl fluorescence parameters.

## Results

**Differences in Chl composition and content between YA-1 yellowish leaves and WT green leaves:** The spectral change of the pigment extract of YA-1 yellowish leaves was the same as that of WT green leaves. The absorption peaks of the pigment extract of WT green leaves were higher than that of YA-1 yellowish leaves. There was a significant difference in pigment content between the two kinds of leaves (Fig. 1). At the seedling stage, the contents of Chl *a*, Chl *b*, and total Chl in YA-1 yellowish leaves were significantly lower than those in WT green leaves, and the Chl content increased gradually with leaf growth. The differences in Chl *a*, Chl *b*, and total Chl contents between yellowish leaves of YA-1 and green leaves at

the same leaf age of WT gradually decreased. When the leaf color of YA-1 yellowish leaves turned green gradually at the bud and blooming stage, there was no significant difference in the contents of Chl *a*, Chl *b*, and total Chl of mature leaves between YA-1 and WT at the same leaf age. The difference in carotenoid content between YA-1 mature leaves and WT green leaves was the same as that of Chl. The ratio of Chl *a* to Chl *b* of YA-1 yellowish leaves was significantly higher than that in WT green leaves, and the ratio of Chl *a* to Chl *b* decreased with the change in leaf color (Table 1). The results show that there were significant differences in pigment content between YA-1 yellowish leaves and WT green leaves.

**Differences in the photosynthetic rate in different growth stages:** At the seedling stage, the net photosynthetic rate ( $P_N$ ), stomatal conductance ( $g_s$ ), and transpiration rate ( $E$ ) of YA-1 yellowish leaves were significantly higher than that of WT green leaves, while the intercellular  $\text{CO}_2$  concentration ( $C_i$ ) was significantly lower than that of WT green leaves (Table 2). At the bud stage, the  $P_N$  of YA-1 yellowish leaves was significantly higher than that of WT green leaves at the same leaf age. The  $C_i$  of YA-1 yellowish leaves was significantly lower than that of WT green leaves. There was no significant difference in  $E$  between YA-1 yellowish leaves and WT green leaves.

**Diurnal variation in the photosynthetic rate:** The  $P_N$ ,  $g_s$ , and  $E$  of YA-1 yellowish leaves and WT green leaves showed a significant correlation with photosynthetic photon flux density (PPFD) during the diurnal variation process. As PPFD increased,  $P_N$ ,  $g_s$ , and  $E$  of YA-1 yellowish leaves and WT green leaves increased (Figs. 2, 3). The diurnal variation of  $P_N$ ,  $g_s$ ,  $C_i$ , and  $E$  of YA-1 yellowish leaves and WT green leaves were the same (Fig. 4). At most time points, the  $P_N$ ,  $g_s$ , and  $E$  of YA-1 yellowish leaves were higher than those of WT green leaves, while there was no obvious difference between the  $C_i$  of YA-1 yellowish leaves and that of WT green leaves.

**Differences in the light response:** In the range of 0–2,000  $\mu\text{mol}(\text{photon}) \text{m}^{-2} \text{s}^{-1}$ , the  $P_N$  of YA-1 yellowish leaves and WT green leaves increased with increasing light intensity. The  $P_N$ ,  $P_{N\text{max}}$ , and  $R_D$  of YA-1 yellowish leaves were higher than those of WT green leaves (Fig. 4A,C,E).

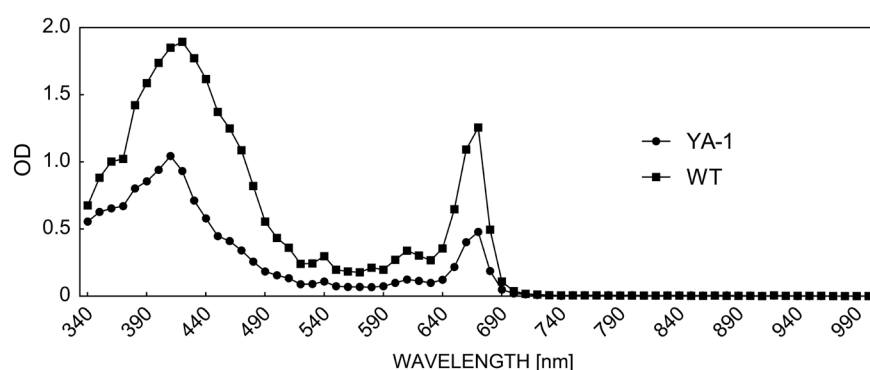


Fig. 1. Spectral scan of 80% acetone pigment extractions. OD – absorbance values.

Table 1. Chlorophyll content of YA-1 yellowish leaves and WT green leaves at different stages. The seedling stage is when two true leaves of a cotton plant are fully unfolded. The bud stage is when cotton plants develop flower buds. The blooming stage is when the cotton plant blooms its first flower. Chl *a* – chlorophyll *a*; Chl *b* – chlorophyll *b*; Chl (*a+b*) – total chlorophyll; Chl *a/b* – the ratio of chlorophyll *a* to chlorophyll *b*. YA-1 young leaves are yellow, WT young leaves are green, and mature leaves of YA-1 and WT are both green. Different letters indicate significant differences ( $p < 0.05$ ).  $n = 5$ .

Stage	Sample	Chl <i>a</i> [mg g <sup>-1</sup> ]	Chl <i>b</i> [mg g <sup>-1</sup> ]	Chl ( <i>a+b</i> ) [mg g <sup>-1</sup> ]	Carotenoid [mg g <sup>-1</sup> ]	Chl <i>a/b</i>
Seedling stage	YA-1 (Young leaves)	0.25 ± 0.07 <sup>b</sup>	0.06 ± 0.02 <sup>b</sup>	0.31 ± 0.09 <sup>b</sup>	0.05 ± 0.02 <sup>b</sup>	4.37 ± 0.19 <sup>a</sup>
	WT (Young leaves)	0.62 ± 0.04 <sup>a</sup>	0.20 ± 0.01 <sup>a</sup>	0.82 ± 0.05 <sup>a</sup>	0.15 ± 0.01 <sup>a</sup>	3.17 ± 0.09 <sup>b</sup>
Bud stage	YA-1 (Mature leaves)	0.68 ± 0.08 <sup>b</sup>	0.19 ± 0.02 <sup>b</sup>	0.87 ± 0.10 <sup>b</sup>	0.16 ± 0.02 <sup>b</sup>	3.54 ± 0.05 <sup>b</sup>
	WT (Mature leaves)	0.80 ± 0.01 <sup>a</sup>	0.23 ± 0.01 <sup>a</sup>	1.03 ± 0.02 <sup>a</sup>	0.19 ± 0.00 <sup>a</sup>	3.47 ± 0.07 <sup>b</sup>
	YA-1 (Young leaves)	0.34 ± 0.03 <sup>c</sup>	0.05 ± 0.01 <sup>c</sup>	0.40 ± 0.04 <sup>c</sup>	0.08 ± 0.01 <sup>c</sup>	6.65 ± 0.68 <sup>a</sup>
	WT (Young leaves)	0.73 ± 0.04 <sup>ab</sup>	0.18 ± 0.01 <sup>b</sup>	0.91 ± 0.06 <sup>b</sup>	0.18 ± 0.01 <sup>ab</sup>	3.97 ± 0.02 <sup>b</sup>
Blooming stage	YA-1 (Mature leaves)	0.84 ± 0.11 <sup>ab</sup>	0.23 ± 0.03 <sup>ab</sup>	1.07 ± 0.14 <sup>ab</sup>	0.17 ± 0.02 <sup>a</sup>	3.59 ± 0.07 <sup>bc</sup>
	WT (Mature leaves)	0.94 ± 0.10 <sup>a</sup>	0.25 ± 0.02 <sup>a</sup>	1.19 ± 0.13 <sup>a</sup>	0.21 ± 0.02 <sup>a</sup>	3.71 ± 0.04 <sup>b</sup>
	YA-1 (Young leaves)	0.34 ± 0.02 <sup>c</sup>	0.06 ± 0.01 <sup>c</sup>	0.40 ± 0.02 <sup>c</sup>	0.11 ± 0.01 <sup>b</sup>	6.12 ± 0.10 <sup>a</sup>
	WT (Young leaves)	0.70 ± 0.06 <sup>b</sup>	0.20 ± 0.02 <sup>b</sup>	0.89 ± 0.08 <sup>b</sup>	0.20 ± 0.02 <sup>a</sup>	3.52 ± 0.03 <sup>c</sup>

Table 2. Photosynthesis parameters of YA-1 and WT leaves. The seedling stage is when two true leaves of a cotton plant are fully unfolded; the bud stage is when cotton plants develop flower buds. YA-1 young leaves are yellow, WT young leaves are green, and mature leaves of YA-1 and WT are both green. Values are means ± SD ( $n = 3$ ). Different lowercase letters denote significant differences at  $P \leq 0.05$ .

Stage	Sample	$P_N$ [ $\mu\text{mol m}^{-2} \text{s}^{-1}$ ]	$g_s$ [ $\text{mmol m}^{-2} \text{s}^{-1}$ ]	$C_i$ [ $\mu\text{mol mol}^{-1}$ ]	$E$ [ $\mu\text{mol m}^{-2} \text{s}^{-1}$ ]
Seedling stage	YA-1 (Young leaves)	22.89 ± 2.20 <sup>a</sup>	0.50 ± 0.06 <sup>a</sup>	297.90 ± 12.80 <sup>b</sup>	4.60 ± 0.47 <sup>a</sup>
	WT (Young leaves)	18.90 ± 1.21 <sup>b</sup>	0.43 ± 0.05 <sup>b</sup>	308.40 ± 11.60 <sup>a</sup>	4.07 ± 0.43 <sup>b</sup>
Bud stage	YA-1 (Young leaves)	22.20 ± 0.38 <sup>a</sup>	0.25 ± 0.05 <sup>a</sup>	258.73 ± 26.83 <sup>a</sup>	4.81 ± 0.51 <sup>a</sup>
	WT (Young leaves)	18.69 ± 1.21 <sup>b</sup>	0.21 ± 0.03 <sup>ab</sup>	262.62 ± 12.70 <sup>a</sup>	4.21 ± 0.48 <sup>a</sup>
	YA-1 (Mature leaves)	16.72 ± 1.46 <sup>b</sup>	0.15 ± 0.01 <sup>b</sup>	114.00 ± 5.23 <sup>b</sup>	3.97 ± 0.41 <sup>a</sup>
	WT (Mature leaves)	14.17 ± 1.52 <sup>c</sup>	0.15 ± 0.06 <sup>b</sup>	141.63 ± 32.09 <sup>b</sup>	3.83 ± 0.68 <sup>a</sup>

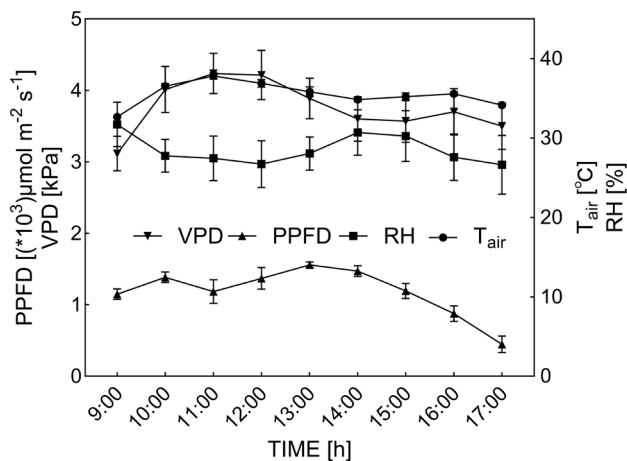


Fig. 2. Diurnal variation of environmental factors. PPFD – photosynthetic photon flux density; RH – relative humidity;  $T_{\text{air}}$  – air temperature; VPD – vapor pressure deficit. Values are means ± SD,  $n = 3$ .

The  $I_m$  and  $I_c$  of YA-1 yellowish leaves were lower than those of WT green leaves (Fig. 4D,F). The  $g_s$  of YA-1 yellowish leaves and WT green leaves increased with

the increase of PPFD, and the  $g_s$  of YA-1 yellowish leaves were higher than those of WT green leaves (Fig. 4B). The yellowish leaves of YA-1 exhibit higher photosynthetic efficiency than those of green leaves of WT at PPFD lower than  $1,500 \mu\text{mol m}^{-2} \text{s}^{-1}$ .

#### The concentration of PEPCase and Rubisco:

The concentration of PEPCase in YA-1 yellowish leaves was 1,314% higher than that of WT leaves. As YA-1 yellowish leaves turned green gradually, the concentration of PEPCase exhibited no significant difference from that in WT green leaves at the same developmental stage. A substantial 91.20% reduction in PEPCase concentration occurred in YA-1 yellowish leaves during the transition from yellow to green (Fig. 5A). The concentration of Rubisco in YA-1 yellowish leaves was 829% higher than that in WT leaves. There was no significant difference between the concentration of Rubisco of YA-1 mature green leaves and WT leaves. A substantial 90% reduction in Rubisco concentration occurred in YA-1 leaves during the transition from yellow to green (Fig. 5B). These results indicate that the concentrations of PEPCase and Rubisco were significantly higher in YA-1 yellowish leaves compared to WT green leaves. However, no significant

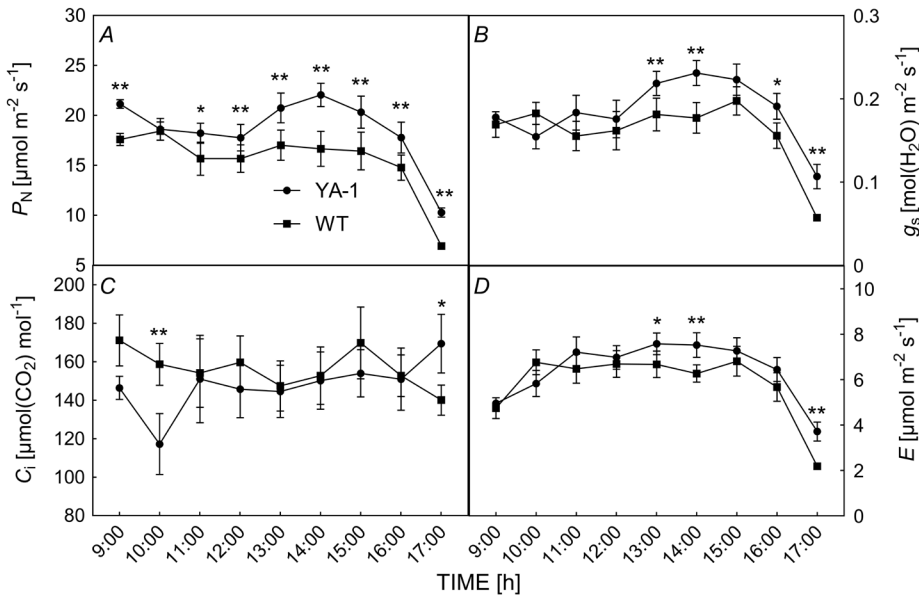


Fig. 3. Diurnal variation in the photosynthetic characteristics of YA-1 yellowish leaves and WT green leaves.  $P_N$  – net photosynthesis rate (A);  $g_s$  – stomatal conductance (B);  $C_i$  – intercellular  $CO_2$  concentration (C);  $E$  – transpiration rate (D). Values are means  $\pm$  SD,  $n = 3$ . \*The difference is significant at the 0.05 level. \*\*The difference is significant at the 0.01 level.

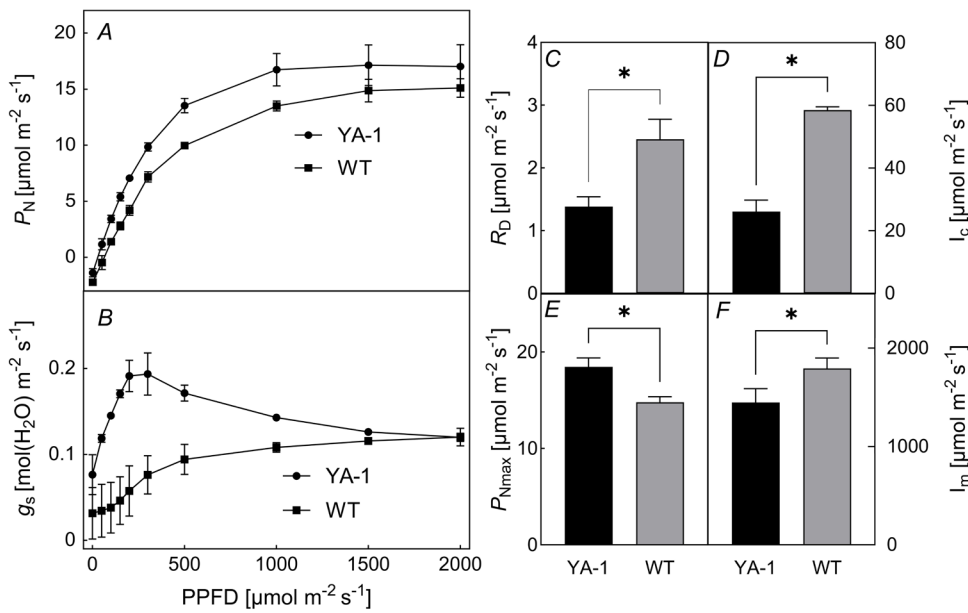


Fig. 4. Light-response curve of YA-1 yellowish leaves and WT green leaves. Light-response curves of the  $P_N$  (A); light-response curves of the  $g_s$  (B);  $R_D$  – dark respiration rate (C);  $I_c$  – light-compensation point (D);  $P_{Nmax}$  – light-saturated net photosynthetic rate (E);  $I_m$  – light-saturation point (F). Values are means  $\pm$  SD,  $n = 3$ . \*The difference is significant at the 0.05 level.

differences in PEPCase or Rubisco concentrations were detected between mature green YA-1 leaves and WT green leaves. During the leaf's color change from yellow to green, the concentrations of two photosynthetic enzymes in YA-1 yellowish leaves were similar to those in WT green leaves, suggesting that the photosynthetic system of YA-1 leaves ultimately returned to a normal level.

**Chl fluorescence parameters:** The  $PI_{abs}$ ,  $F_v/F_m$ , and  $F_v/F_0$  of YA-1 yellowish leaves were higher than those of WT

green leaves (Fig. 2SA,B,D; *supplement*), while the  $F_0$  and  $F_m$  of YA-1 yellowish leaves were lower than those of WT green leaves (Fig. 2SC,E). The maximum photochemical efficiency, potential photochemical activity, and light-energy utilization efficiency of YA-1 yellowish leaves were higher than that of WT green leaves, and the degree of minimal fluorescence and maximal fluorescence was lower than that of WT leaves. The  $PI_{abs}$ ,  $F_v/F_m$ , and  $F_v/F_0$  of YA-1 yellowish leaves and WT leaves showed a downward trend (Fig. 2SA,B,D), while  $F_0$  and  $F_m$  showed

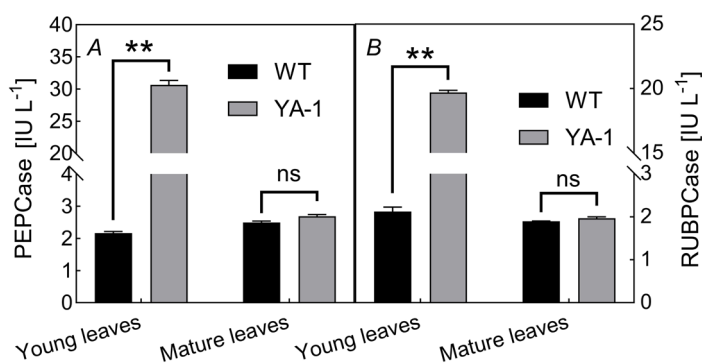


Fig. 5. Quantitative determination of PEPCase and Rubisco concentrations in YA-1 yellowish and WT green leaves. Quantitative determination of PEPCase (A); quantitative determination of Rubisco (B). \*\*The difference is significant at the 0.01 level; ns indicate that the data comparison difference is not significant.  $n = 3$ .

an upward trend at different growth stages (Fig. 2SC,E), indicating that photosynthetic performance, maximum photochemical efficiency, potential photochemical activity, and light-energy utilization efficiency of YA-1 and WT leaves gradually decreased, while the degree of minimal fluorescence and maximal fluorescence gradually increased with the maturity of leaves.

**PSII reaction center activity:** The  $ABS/RC$ ,  $TR_0/RC$ ,  $ET_0/RC$ , and  $DI_0/RC$  of YA-1 yellowish leaves were lower than that of WT green leaves (Fig. 2SF–J), which indicated that the light energy absorbed by unit reaction centers, the energy captured to reduce  $Q_A$ , the energy of electron transfer, and the energy dissipated by heat in YA-1 yellowish leaves were lower than that of WT green leaves. These parameters increased with the growth of leaves. The activity of the PSII reaction center in YA-1 yellowish leaves was lower than that of WT green leaves. With the yellowish leaves turning green gradually, the activity of the PSII reaction center increased, which was consistent with that in WT leaves. Compared to WT green leaves, YA-1 yellowish leaves exhibited lower light energy utilization and energy transfer efficiency at the PSII reaction center.

**The difference of PSII energy distribution ratio:**

The electron energy captured by reaction center ( $PSI_0$ ), maximum photochemical efficiency [ $\Phi(P_0)$ ], and photochemical reaction efficiency [ $\Phi(E_0)$ ] of YA-1 yellowish leaves were higher than that of WT green leaves (Fig. 2SJ–L), while the quantum ratio of heat dissipation [ $\Phi(D_0)$ ] was lower than that of WT green leaves (Fig. 2SM), which indicated that the proportion of the energy captured by  $Q_A$  to the captured energy of the reaction center when the trapped electron passes through  $Q_A$ , maximum photochemical efficiency, and quantum yield for electron transport of YA-1 yellowish leaves were higher than those of WT green leaves, and the quantum ratio of heat dissipation was lower than that of WT leaves. The  $PSI_0$ ,  $\Phi(P_0)$ , and  $\Phi(E_0)$  values of YA-1 yellowish leaves showed a decreasing trend compared to WT green leaves (Fig. 2SJ–L). With the leaves turned gradually green, the differences in these parameters between YA-1 yellowish leaves and WT green leaves gradually decreased, and quantum ratio of PSII for heat dissipation gradually increased. The PSII energy allocation ratio of

YA-1 yellowish leaves was higher than that of WT leaves. As the leaves gradually turned green, the PSII energy allocation ratio decreased. YA-1 yellowish leaves exhibited superior light energy capture, maximum photochemical efficiency, and electron transfer compared to WT green leaves. YA-1 compensated for the limitations in light energy utilization through efficient light energy absorption and electron transfer, thereby enhancing its photosynthetic capacity.

**PSII light energy-utilization efficiency:** The light energy captured per unit area ( $TR_0/CS_0$ ), absorption flux per unit area ( $ABS/CS_0$ ), quantum yield of electron transfer per unit area ( $ET_0/CS_0$ ), and heat dissipation per unit area ( $DI_0/CS_0$ ) of YA-1 yellowish leaves were lower than those of WT green leaves (Fig. 2SF–J), indicating that the light energy captured, absorbed, quantum yield of electron transfer, and heat dissipation per unit area of YA-1 yellowish leaves was lower than those of WT green leaves.  $TR_0/CS_0$ ,  $ABS/CS_0$ , and  $DI_0/CS_0$  of YA-1 yellowish leaves and WT green leaves increased at different growth stages (Fig. 2SO,P,R), while  $ET_0/CS_0$  increased at first and then decreased (Fig. 2SQ), indicating that with the gradual maturity of leaves, the light energy captured, absorbed, used for electron transport and heat dissipation per unit area of YA-1 yellowish leaves and WT green leaves gradually increased. In contrast, the light energy used for electron transfer increased at first and then decreased. The light energy-utilization efficiency of PSII of YA-1 yellowish leaves was lower than that of WT green leaves. With the yellowish leaves turning green gradually, the light energy-utilization efficiency of PSII increased, which was consistent with that of WT green leaves.

The  $RC/CS_0$  of YA-1 yellowish leaves and WT green leaves changed little in different growth stages (Fig. 2SN), with no significant difference in the number of active reaction centers per unit area between YA-1 yellowish leaves and WT green leaves.

**GO pathway enrichment analysis of DEGs:** A total of 4,002 DEGs were upregulated and 2,766 DEGs were downregulated between YA-1 yellowish leaves and WT green leaves (Table 3S, supplement; Fig. 3S, supplement). A total of 215 significantly enriched GO terms were obtained after screening (Table 4S, supplement), the DNA binding pathway has the most enriched DEGs in GO, followed by the nucleus pathway (Fig. 4S, supplement).

**KEGG pathway enrichment analysis of DEGs:** A total of 2,784 DEGs between YA-1 yellowish leaves and WT green leaves were annotated into 134 KEGG pathways (Table 5S, *supplement*). These pathways included porphyrin and Chl metabolism, carotenoid biosynthesis, flavonoid biosynthesis, phenylpropanoid biosynthesis, and anthocyanin biosynthesis, and other pathways related to the leaf color pathway, photosynthesis, photosynthesis-antenna proteins, and carbon fixation in photosynthetic organisms (Table 6S, *supplement*).

**DEGs related to photosynthetic pigment metabolism:**

The five metabolic pathways related to leaf color and 218 DEGs were enriched. In the pathway of porphyrin and Chl metabolism, there were 3 DEGs, 2 upregulated [encoding magnesium dechelatease (SGRL) and chlorophyllide *a* oxygenase (CAO)] and 1 downregulated [encoding glutamate-1-semialdehyde 2,1-aminomutase (HemL)]. There were 23 DEGs, 12 upregulated and 11 downregulated in the carotenoid biosynthesis pathway, which mainly encode xanthoxin dehydrogenase (ABA2), 9-cis-epoxy carotenoid dioxygenase (NCED), and momilactone-A synthase (MAS). There were 7 DEGs, 4 upregulated and 3 downregulated in the anthocyanin biosynthesis pathway, which encode 5,3-O-glucosyltransferase (GT1) and 3-O-glucosyltransferase (BZ1) (Table 7S, *supplement*). The 41 DEGs enriched in the flavonoid biosynthesis pathway were identified, of which 26 DEGs were upregulated and 15 DEGs were downregulated. The 9 DEGs were upregulated and 1 DEG was downregulated among the genes encoding hydroxycinnamoyl transferase (HCT), 7 were upregulated and 3 were downregulated among the genes encoding flavonol synthase (FLS). Other DEGs encode chalcone synthase (CHS), flavin-containing monooxygenase (FMO), anthocyanidin reductase (ANR), anthocyanidin synthase (ANS), bifunctional dihydroflavonol 4-reductase/flavanone 4-reductase (DFR), omega-hydroxy palmitate O-feruloyl transferase (HHT1), and so on (Table 7S).

Phenylpropanoid is the precursor of anthocyanin biosynthesis, and the DEGs in the phenylpropanoid biosynthesis pathway may be the reason for the color change of YA-1 yellowish leaves. Of a total of 144 DEGs, 99 were upregulated and 45 were downregulated in the phenylpropanoid biosynthesis pathway. The genes enriched in the phenylpropanoid biosynthesis pathway mainly encode peroxidase (POD),  $\beta$ -glucosidase, 2,4-dihydroxy-1,4-benzoxazin-3-one-glucoside dioxygenase (BX6), E3 ubiquitin-protein ligase (UBR4), and phenylalanine ammonia lyase (PAL). These genes play roles in different stages of the phenylpropanoid biosynthesis pathway, and there was a significant difference in transcription between YA-1 yellowish leaves and wild-type green leaves. The genes encoding 4-coumarate-CoA ligase (4CL), cinnamyl-alcohol dehydrogenase (CAD), and cinnamyl-CoA reductase (CCR) were also differentially expressed in the phenylpropane synthesis pathway, and there was a significant difference in transcription between YA-1 yellowish leaves and WT green leaves (Table 7S). The transcriptome results showed that the formation

of YA-1 yellowish leaves was related to the biosynthesis of Chl, carotenoids, and anthocyanins. Phenylpropanoids and flavonoids, as precursors of anthocyanin biosynthesis, may be involved in the formation of YA-1 yellowish leaves.

**DEGs related to photosynthesis metabolism:**

The difference in pigments directly affected the state of chloroplasts and plant photosynthesis. There were 16 DEGs in the photosynthesis pathway, involving PSI, PSII, the cytochrome *b<sub>6</sub>/f* complex, the photosynthetic electron transport chain, and F-type ATP enzymes. Six were upregulated, and 10 were downregulated in YA-1 yellowish leaves. There were 3 DEGs in the photosynthetic antenna protein pathway, 2 DEGs upregulated, and 1 DEG of YA-1 yellowish leaves downregulated (Table 8S, *supplement*). A total of 24 DEGs were enriched in the carbon fixation pathway of photosynthetic organs, of which 10 DEGs were upregulated and 14 DEGs were downregulated, such as encoding glyceraldehyde 3-phosphate dehydrogenase (GAPDH), fructose-bisphosphate aldolase (ALDO), malate dehydrogenase (MDH), ribose-5-phosphate isomerase A (rpiA), alanine transaminase (GPT), pyruvate orthophosphate dikinase (PPDK), ribulose-phosphate 3-epimerase (RPE), triosephosphate isomerase (TPI), and phosphoglycerate kinase (PGK), respectively (Table 8S).

**Genes related to Chl synthesis and metabolism in YA-1 yellowish leaves:**

HemL, SGRL, and CAO encoded by *GhHemL*, *GhSGRL*, and *GhCAO* involve in the regulation of Chl biosynthesis (Fig. 6A). HemL participates in the conversion of L-glutamic acid-tRNA to aminolevulinic acid (ALA), which is in the upstream of the Chl synthesis pathway. The genes encoding this substance in the yellowish leaves of YA-1 were downregulated, which directly affected the synthesis of ALA, and then hindered the synthesis of Chl in the yellowish leaves of YA-1. With the transformation of YA-1 leaves from yellow to green, the relative expression of *GhHemL* increased gradually, which promoted the synthesis and transformation of ALA, and Chl synthesis in YA-1 leaves was promoted (Fig. 6A). SGRL catalyzes the conversion of chlorophyllin *a* to pheophorbide *a* and the degradation of Chl *a* to demagnesium chlorophyll *a*, which plays an important role in the degradation of Chl *a*. The downregulated expression of *GhSGRL* in the yellowish leaves of YA-1 affected the degradation of Chl *a* in the yellowish leaves of YA-1. During YA-1 yellowish leaves turn into green (S1–S4), the relative expression of *GhSGRL* increased gradually, which promoted the degradation of Chl *a* in YA-1 yellowish leaves (Fig. 6A,B).

CAO catalyzes the conversion of chlorophyllin *a* to chlorophyllin *b*, which is a key step in the synthesis of Chl *b*. The downregulation of *GhCAO* expression in YA-1 yellowish leaves affected the synthesis of Chl *b* in YA-1 yellowish leaves. As YA-1 yellowish leaves turned green, the relative expression of *GhCAO* increased and the conversion of chlorophyllin *a* to chlorophyllin *b* was promoted, thus promoting the synthesis of Chl *b* in YA-1 yellowish leaves (Fig. 6A,B). HemL, SGRL, and CAO

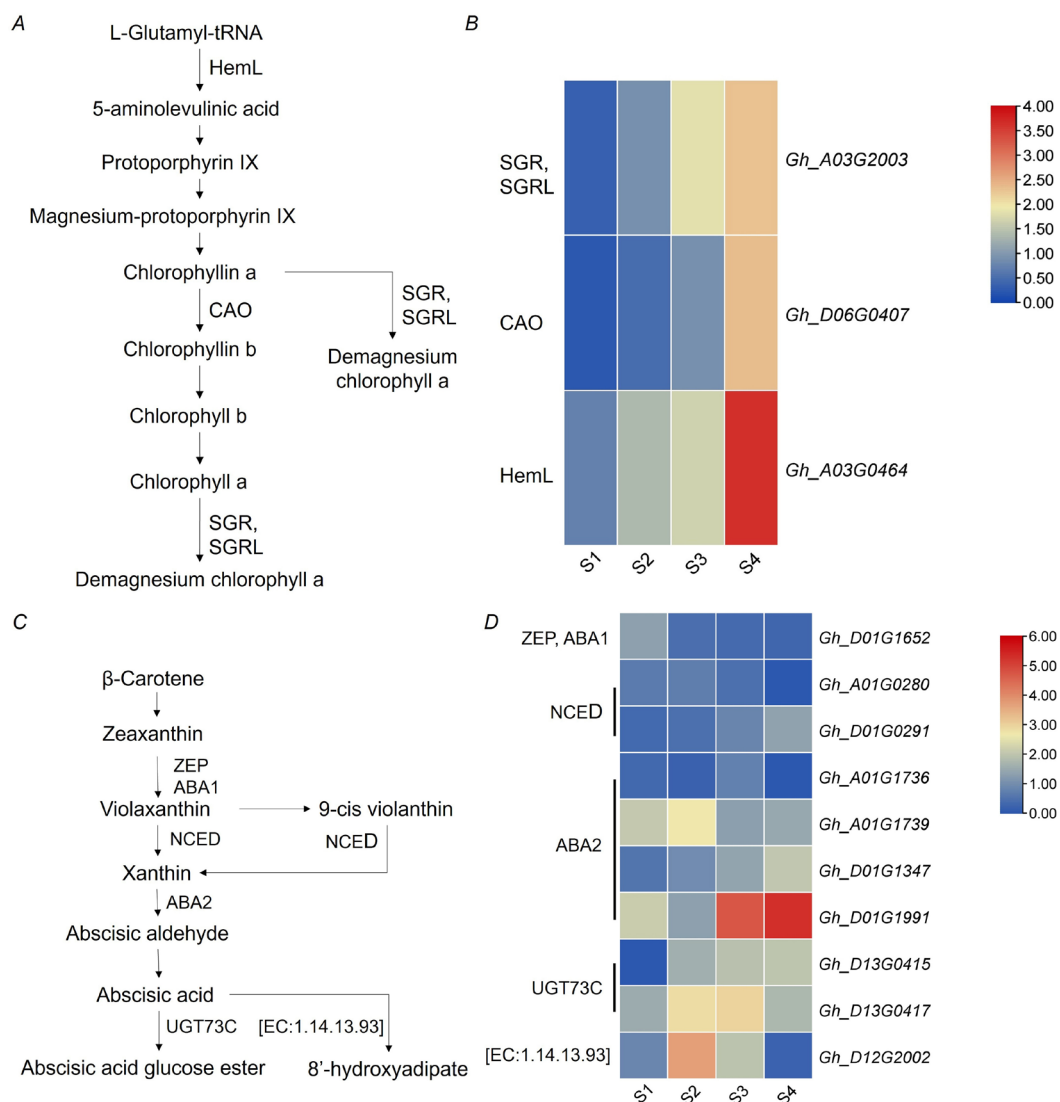


Fig. 6. Pigment synthesis pathway and dynamic expression analysis of related genes. Chlorophyll anabolic pathway (A); expression heatmap of genes related to chlorophyll synthesis metabolism pathway (B); carotenoid anabolic pathway (C); expression heatmap of genes related to carotenoid anabolic pathway (D). S1–S4: S1 is the period when the first real leaf fully unfolds and then samples are taken every 7 d for a total of four times, S1–S4 represents the period of four sampling sessions. ABA2 – xanthoxin dehydrogenase; SGR, SGRL – magnesium dechelatease; CAO – chlorophyllide *a* oxygenase; HemL – glutamate-1-semialdehyde 2,1-aminomutase; NCED – 9-cis-epoxycarotenoid dioxygenase; ZEP (ABA1) – zeaxanthin epoxidase; UGT73C – glucosyltransferase; EC 1.14.13.93 – (+)-abscisic acid 8'-hydroxylase. *n* = 3.

regulated the synthesis of total Chl and its components in yellowish leaves of YA-1. The relative expression of *GhHemL*, *GhSGRL*, and *GhCAO* affected the changes in Chl content and components in yellowish leaves of YA-1.

**DEGs related to carotenoid metabolism in YA-1 yellowish leaves:** Zeaxanthin epoxidase (ZEP, ABA1), NCED, ABA2, glucosyltransferase (UGT73C), and (+)-abscisic acid 8'-hydroxylase encoded by *GhZEP*, *GhNCED*, *GhABA2*, *GhUGT73C*, and EC 1.14.13.93 are involved in the regulation of carotenoid biosynthesis. ZEP (ABA1) is involved in the conversion of zeaxanthin to violaxanthin, a decomposition product of β-carotene. NCED is involved in the regulation of the conversion of

violaxanthin to flaxanthin and 9-cis-violaxanthin to lutein. ABA2 catalyzes the conversion of xanthin to abscisic aldehyde. UGT73C and (+)-abscisic acid 8'-hydroxylase catalyze the conversion of abscisic acid to glucose abscisic acid ester and 8-hydroxyadipate, respectively (Fig. 6C). During the process of YA-1 yellowish leaves change into green, samples were collected from four periods (S1, S2, S3, S4). At the S1, *GhZEP* in YA-1 yellowish leaves was upregulated, which promoted the transformation of zeaxanthin into violaxanthin, which is the decomposition product of β-carotene, and regulated the decomposition of carotenoid pigments and β-carotene. At the S1, the expression of *GhNCED* in YA-1 yellowish leaves was downregulated, which affected

the decomposition of violaxanthin in YA-1 yellowish leaves. The expression of genes encoded ZEP and NCED catalyze the synthesis of violaxanthin in YA-1 yellowish leaves, block the decomposition reaction, and accumulated violaxanthin in YA-1 yellowish leaves. At the same time, substances involved in downstream reactions in this pathway, such as ABA2, UGT73C, and (+)-abscisic acid 8'-hydroxylase, are inconsistently expressed as upregulated and downregulated in YA-1 yellowish leaves, which may be due to their involvement in other biochemical reactions such as abscisic acid synthesis in YA-1 yellowish leaves (Fig. 6D). With the yellowish leaves of YA-1 changed into green (S1–S4), the expression of *GhZEP* involved in the upstream reaction of  $\beta$ -carotene decomposition decreased, which hindered the  $\beta$ -carotene decomposition reaction from upstream, and carotenoid pigments accumulated in YA-1 yellowish leaves. The relative expression of genes encoded by the substances involved in the downstream reaction in this pathway had little effect on the accumulation of carotenoid pigments (Fig. 6C,D).

The upregulation of *GhZEP* involved in the upstream reaction promoted the decomposition of  $\beta$ -carotene, and the accumulation of carotenoid pigments in yellowish leaves of YA-1 was blocked. During the transition from yellow to green, the decomposition of  $\beta$ -carotene in YA-1 was blocked and carotenoid pigments in YA-1 leaves accumulated due to the downregulation of *GhZEP*.

## Discussion

**The gradual decrease in Chl *a/b* leads to the transformation of YA-1 from yellow to green:** YA-1 yellowish leaves exhibited significantly lower contents of Chl *a*, Chl *b*, carotenoids, and total Chl content compared to WT green leaves. This reduction in Chl content is one of the key factors contributing to the yellowish appearance of YA-1 leaves. Similar to our results, the relative content of *Anthurium andraeanum* 'Sonate' pigments can change leaf color (Yang *et al.* 2015). The yellow-green leaf mutant of birch contained less Chl and carotenoids (Gang *et al.* 2019). The ratio of Chl *a* to Chl *b* in YA-1 yellowish leaves was significantly higher than that in WT, suggesting a shift in the Chl composition during the yellowing process. Consistently with our findings, the Chl *a/b* ratio of the rice virescent mutant *yg18* was altered (Zhu *et al.* 2016).

With the growth of leaves, the pigment difference between YA-1 and WT leaves decreased. During the transition from yellow to green leaves in YA-1, the expression of *GhHemL*, *ChSGRL*, and *GhCAO* gradually increased. The expression of these genes of YA-1 yellowish leaves was downregulated. Consistent with the findings of this study, downregulation of *HemL* expression has been shown to reduce Chl content in rapeseed (Tsang *et al.* 2003), the decrease in *OsCAO* expression in the rice yellow-green leaf mutant *yg110* resulted in much lower Chl *b* content (Yang *et al.* 2014). *OsSGR* regulates Chl degradation at the transcriptional level (Park *et al.* 2007, Matsuda *et al.* 2016, Shimoda *et al.* 2016). The downregulation of *GhHemL*, *ChSGRL*, and *GhCAO* expression in YA-1 yellowish leaves may contribute to the significant reduction in Chl *a*, Chl *b*,

and total Chl content, leading to the chlorosis observed in YA-1 yellowish leaves compared to WT green leaves.

In the carotenoid biosynthesis pathway, *GhZEP* and *GhNCED* were significantly differentially expressed. During the transition from yellowish to green leaves in YA-1, the expression of *GhZEP* gradually decreased, while *GhNCED* expression gradually increased. The high expression of the zeaxanthin cyclooxygenase gene *ZEP* accelerates the transformation of  $\beta$ -carotene to antheraxanthin and violaxanthin, and *ZEP* participates in the downstream pathway of  $\beta$ -carotene biosynthesis (Sun *et al.* 2022). The upregulated expression of *GhZEP* in YA-1 yellowish leaves may promote the reaction after  $\beta$ -carotene transformation and affect the accumulation of carotenoids in leaves. With YA-1 yellowish leaves changed into green, the expression of *GhZEP* decreased gradually, which slowed the decomposition and transformation of  $\beta$ -carotene, and carotenoids accumulated in the green leaves of YA-1.

In the anthocyanin biosynthesis pathway, *Gh3GT* was significantly upregulated in the yellowish leaves of YA-1. Anthocyanin 3-O-glucosyltransferase (3GT), as the last step of anthocyanin glycoside synthesis, catalyzes unstable anthocyanin to anthocyanin glycoside (Du *et al.* 2017). Anthocyanins originate from a branch of the flavonoid pathway, which begins with phenylalanine via the phenylpropane pathway (Falcone Ferreyra *et al.* 2012, Guo *et al.* 2019, Gao *et al.* 2020). In the phenylpropane biosynthesis pathway of YA-1 yellowish leaves, both *PAL* and *4CL* showed differential expression. The phenylpropane biosynthesis pathway contains three main genes, such as *PAL*, *C4H* (cinnamic acid-4-hydroxylase), and *4CL*, the expression abundance of *CHS*, *F3H* (naringenin 3-dioxygenase), *DFR*, and *GTI* also controls the biosynthesis of phenylpropane (Falcone Ferreyra *et al.* 2012). The genes encoding COMT (caffeic acid 3-O-methyltransferase/acetylserotonin O-methyltransferase), such as *CAD*, *GTI*, *FMO*, and *CCR* were identified. A large number of genes related to leaf color were also detected in the flavonoid biosynthesis pathway, including *PAL*, *CHS*, *ANS*, *UFGT*, *FLS*, *C4H*, *4CL*, *DFR*, and *ANR* (He *et al.* 2010, Song *et al.* 2020). The genes encoding *FLS*, *CHS*, *F3H*, *ANR*, *DFR*, and *ANS* were differentially expressed in the yellowish leaves of YA-1, and genes encoding *FMO* and *LAR* (leucoanthocyanidin reductase) were also identified. The biosynthesis of phenylpropane and flavonoids may be affected by the differential expression genes of the phenylpropane and flavonoid biosynthesis pathways and affect anthocyanin synthesis.

**The high *g*, *E*, and low *I<sub>m</sub>*, *I<sub>c</sub>* led to high *P<sub>N</sub>* of YA-1 yellowish leaves:** The *P<sub>N</sub>*, *g<sub>s</sub>*, and *E* of YA-1 yellowish leaves were significantly higher than those of WT leaves, *I<sub>c</sub>* and *I<sub>m</sub>* were significantly lower than WT leaves, the *C<sub>i</sub>* of YA-1 yellowish leaves was not significantly different than WT leaves. The chloroplast-deficient yellow leaf mutants of watermelon, *P<sub>N</sub>* and *E* were significantly lower, while *g<sub>s</sub>* and *C<sub>i</sub>* were higher than those of WT (Xu *et al.* 2023). The yellow-green leaves of Jimai (*Triticum aestivum*)

exhibited higher  $I_c$  and  $I_m$  than WT (Zheng *et al.* 2021). Our results are not consistent with those of Xu *et al.* (2023) and Zheng *et al.* (2021). The elevated  $g_s$  enables YA-1 yellowish leaves to sustain efficient transpiration and carbon fixation even under high PPFD. Higher  $g_s$ ,  $E$  and lower  $I_m$ ,  $I_c$  of YA-1 yellowish leaves led to higher  $P_N$  than WT green leaves, which may compensate for reduced pigment concentration.

**The high concentrations of Rubisco and PEPCase led to high  $P_N$  of YA-1 yellowish leaves:** The concentrations of Rubisco and PEPCase in YA-1 yellowish leaves were significantly higher than those of wild type green leaves. The concentration of Rubisco is positively correlated with photosynthetic rate (Scafarò *et al.* 2023). The concentration of PEPCase carboxylase is usually related to the photosynthetic capacity of plants, and its changes affect the rate of photosynthetic processes (Doubnerová and Ryšlavá 2011). These enzymes are involved in carbon fixation and Calvin cycle, which may be the important factors leading to the  $P_N$  enhancement of YA-1 yellowish leaves.

**The high  $F_v/F_m$ ,  $PI_{abs}$ ,  $PSI_0$ ,  $PHI(P_0)$ ,  $PHI(E_0)$ , and low  $DI_0/RC$ ,  $DI_0/CS_0$ ,  $DI_0/CS_m$  led to high  $P_N$  of YA-1 yellowish leaves:** The higher  $F_v/F_m$ ,  $PI_{abs}$ ,  $PSI_0$ ,  $PHI(P_0)$ ,  $PHI(E_0)$  and lower  $DI_0/RC$ ,  $DI_0/CS_0$ ,  $DI_0/CS_m$  of YA-1 yellowish leaves indicate that YA-1 yellowish leaves maintained high PSII photochemical efficiency, light absorption capacity, and energy utilization efficiency while reducing heat dissipation. These changes are directly associated with the  $P_N$  increase of YA-1 yellowish leaves compared to WT green leaves.  $P_N$  of upland cotton is positively correlated with  $F_v/F_m$  and  $PI_{abs}$  (Zhou *et al.* 2021). Our results indicate that high  $F_v/F_m$ ,  $PI_{abs}$ ,  $PSI_0$ ,  $PHI(P_0)$ , and  $PHI(E_0)$  relate to high  $P_N$ . These results suggest that energy absorption alone is not the primary determinant of  $P_N$ , the efficiency of energy allocation may play a critical role in regulating photosynthesis of YA-1 yellowish leaves.

**DEGs of photosynthesis and pigment pathway led to high  $P_N$  of YA-1 yellowish leaves:** In photosynthesis pathway, the downregulation of *GhPsbC* and *GhPsbB* and the upregulation of *GhPsbS* expression in YA-1 yellowish leaves were found. *Psb[A-F]* encodes the core component of PSII (Jiang *et al.* 2020). *PsbS* is a photoprotective protein on the thylakoid membrane and plays a key role in the mechanism of high light protection (Fan *et al.* 2015). The downregulation of *GhPsbC* and *GhPsbB* and the upregulation of *GhPsbS* expression may affect the activity of PSII, and result in a decrease in light energy absorption of YA-1 yellowish leaves. In photosynthesis-antenna proteins pathway, *GhLHCB4* and *GhLHCB5*, which encode LHCII chlorophyll *a/b*-binding protein LHC 4 and LHC 5, were upregulated in YA-1 yellowish leaves, while *GhLHCB6*, encoding LHC II chlorophyll *a/b*-binding protein LHC 6, was downregulated. *LHCB4*, *LHCB5*, and *LHCB6* play an important role in light capture and energy dissipation (Andersson *et al.* 2001, Bianchi

*et al.* 2008, Sun *et al.* 2022, Levin and Schuster 2023). The  $P_N$  of YA-1 yellowish leaves was higher than that of the WT green leaves, and the differential expression of LHC family genes may be related to the photosynthetic rate.

**The application of YA-1 in upland cotton hybrid seeds production:** YA-1 is a genic male sterility line characterized by yellowish young leaves, with a 1:1 ratio of male sterility to male fertility plants (msms:Msms). The 50% male sterile plants can be used as female parents for crossing with all upland cotton varieties with green leaves, while the 50% fertile plants can be removed prior to hybridization. This approach enables the selection of high-quality F1 hybrids and the large-scale production of commercial hybrid seeds. Additionally, any false F1 seedlings resulting from the selfing of residual fertile plants can be identified and eliminated. This strategy offers a significant advantage compared to genic male sterility lines with green leaves. In this study, the photosynthetic rate of YA-1 yellowish leaves did not negatively impact the overall photosynthetic efficiency. Furthermore, the photosynthetic rate of F1 hybrids between YA-1 and upland cotton cultivars (Vv) was unlikely to be adversely affected. However, further investigations are needed to fully assess this problem.

**Conclusion:** The decreased content of Chl, carotenoids and increased proportion of Chl *a/b* led to the yellowish phenotype of YA-1. The decreased expression of the *GhHemL*, *GhCAO*, and *GhSGRL* genes hinder the synthesis of chlorophyll, and the decreased expression of *GhZEP* and *GhNCED* block the synthesis of carotenoids, increase the proportion of photosynthetic pigments in YA-1 and produce yellowish leaves. YA-1 yellowish leaves show high  $P_N$ ,  $g_s$ ,  $F_v/F_m$ ,  $PI_{abs}$ ,  $PSI_0$ ,  $PHI(P_0)$ ,  $PHI(E_0)$ , and concentrations of Rubisco and PEPCase. The differential expression of *GhPsbB*, *GhPsbC*, *GhPsbS*, *GhLHCB4*, *GhLHCB5*, and *GhLHCB6* in photosynthesis and the photosynthetic-antenna protein pathway results in higher  $P_N$  in YA-1 yellowish leaves than those of WT. The yellowish leaves of YA-1 can serve as a distinct marker trait in breeding programs without compromising photosynthetic efficiency.

## References

- Andersson J., Walters R.G., Horton P., Jansson S.: Antisense inhibition of the photosynthetic antenna proteins CP29 and CP26: implications for the mechanism of protective energy dissipation. – *Plant Cell* **13**: 1193-1204, 2001.
- Bianchi S., Dall'Osto L., Tognon G. *et al.*: Minor antenna proteins CP24 and CP26 affect the interactions between photosystem II subunits and the electron transport rate in grana membranes of *Arabidopsis*. – *Plant Cell* **20**: 1012-1028, 2008.
- Doubnerová V., Ryšlavá H.: What can enzymes of  $C_4$  photosynthesis do for  $C_3$  plants under stress? – *Plant Sci.* **180**: 575-583, 2011.
- Du L.J., Chen K.L., Liu Y.L.: [Cloning and expression analysis of anthocyanidin 3-O-glucosyltransferase gene in grape hyacinth.] – *Pratacult. Sci.* **34**: 2235-2244, 2017. [In Chinese]

- Falcone Ferreyra M.L., Rius S.P., Casati P.: Flavonoids: biosynthesis, biological functions, and biotechnological applications. – *Front. Plant Sci.* **3**: 222, 2012.
- Fan L., Hou Y., Zheng L. *et al.*: Characterization and fine mapping of a yellow leaf gene regulating chlorophyll biosynthesis and chloroplast development in cotton (*Gossypium arboreum*). – *Gene* **885**: 147712, 2023.
- Fan M., Li M., Liu Z. *et al.*: Crystal structures of the PsbS protein essential for photoprotection in plants. – *Nat. Struct. Mol. Biol.* **22**: 729-735, 2015.
- Gang H., Liu G., Chen S., Jiang J.: Physiological and transcriptome analysis of a yellow-green leaf mutant in birch (*Betula platyphylla* × *B. pendula*). – *Forests* **10**: 120, 2019.
- Gao J., Ren R., Wei Y. *et al.*: Comparative metabolomic analysis reveals distinct flavonoid biosynthesis regulation for leaf color development of *Cymbidium sinense* 'Red Sun'. – *Int. J. Mol. Sci.* **21**: 1869, 2020.
- Guo N., Han S., Zong M. *et al.*: Identification and differential expression analysis of anthocyanin biosynthetic genes in leaf color variants of ornamental kale. – *BMC Genomics* **20**: 564, 2019.
- He F., Mu L., Yan G.-L. *et al.*: Biosynthesis of anthocyanins and their regulation in colored grapes. – *Molecules* **15**: 9057-9091, 2010.
- Jiang Y., Wang Q., Shen Q.-Q. *et al.*: Transcriptome analysis reveals genes associated with leaf color mutants in *Cymbidium longibracteatum*. – *Tree Genet. Genom.* **16**: 44, 2020.
- Levin G., Schuster G.: LHC-like proteins: the guardians of photosynthesis. – *Int. J. Mol. Sci.* **24**: 2503, 2023.
- Li W.-X., Yang S.-B., Lu Z.-G. *et al.*: Cytological, physiological, and transcriptomic analyses of golden leaf coloration in *Ginkgo biloba* L. – *Hortic. Res.* **5**: 12, 2018.
- Mao G., Ma Q., Wei H. *et al.*: Fine mapping and candidate gene analysis of the virescent gene *v1* in upland cotton (*Gossypium hirsutum*). – *Mol. Genet. Genomics* **293**: 249-264, 2018.
- Mao G., Wei H., Hu W. *et al.*: Fine mapping and molecular characterization of the virescent gene *vsp* in upland cotton (*Gossypium hirsutum*). – *Theor. Appl. Genet.* **132**: 2069-2086, 2019.
- Matsuda K., Shimoda Y., Tanaka A., Ito H.: Chlorophyll *a* is a favorable substrate for *Chlamydomonas* Mg-dechelataase encoded by *STAY-GREEN*. – *Plant Physiol. Biochem.* **109**: 365-373, 2016.
- Park S.-Y., Yu J.-W., Park J.-S. *et al.*: The senescence-induced staygreen protein regulates chlorophyll degradation. – *Plant Cell* **19**: 1649-1664, 2007.
- Scafaro A.P., Posch B.C., Evans J.R. *et al.*: Rubisco deactivation and chloroplast electron transport rates co-limit photosynthesis above optimal leaf temperature in terrestrial plants. – *Nat. Commun.* **14**: 2820, 2023.
- Shimoda Y., Ito H., Tanaka A.: *Arabidopsis STAY-GREEN*, Mendel's green cotyledon gene, encodes magnesium-dechelataase. – *Plant Cell* **28**: 2147-2160, 2016.
- Song B., Xu H., Chen L. *et al.*: Study of the relationship between leaf color formation and anthocyanin metabolism among different purple pakchoi lines. – *Molecules* **25**: 4809, 2020.
- Song M.M., Fan S.L., Pang C.Y. *et al.*: [Research on the main photosynthetic characteristics and agronomic traits in virescent cotton materials.] – *Cotton Sci.* **26**: 531-538, 2014. [In Chinese]
- Song M.Z., Yang Z.G., Fan S.L. *et al.*: [Physiological and biochemical analysis and identification of a short season cotton virescent mutant.] – *Sci. Agr. Sin.* **44**: 3709-3720, 2011. [In Chinese]
- Song M.Z., Yang Z.G., Fan S.L. *et al.*: Cytological and genetic analysis of a virescent mutant in upland cotton (*Gossypium hirsutum*). – *Euphytica* **187**: 235-245, 2012.
- Sun Y., Bai P.-P., Gu K.-J. *et al.*: Dynamic transcriptome and network-based analysis of yellow leaf mutant *Ginkgo biloba*. – *BMC Plant Biol.* **22**: 465, 2022.
- Tsang E.W.T., Yang J., Chang Q. *et al.*: Chlorophyll reduction in the seed of *Brassica napus* with a glutamate 1-semialdehyde aminotransferase antisense gene. – *Plant Mol. Biol.* **51**: 191-201, 2003.
- Wang X.K., Huang J.L.: Principles and Techniques of Plant Physiological and Biochemical Experiments. 3<sup>rd</sup> Edition. Pp. 324. Higher Education Press, Beijing 2015.
- Xu B., Zhang C., Gu Y. *et al.*: Physiological and transcriptomic analysis of a yellow leaf mutant in watermelon. – *Sci. Rep.-UK* **13**: 9647, 2023.
- Yang H.L., Liu M., Guo J. *et al.*: [Genetic analysis and position cloning of a yellow-green leaf 10 (*yg110*) gene, responsible for leaf color in rice.] – *Chin. J. Rice Sci.* **28**: 41-48, 2014. [In Chinese]
- Yang Y., Chen X., Xu B. *et al.*: Phenotype and transcriptome analysis reveals chloroplast development and pigment biosynthesis together influenced the leaf color formation in mutants of *Anthurium andraeanum* 'Sonate'. – *Front. Plant Sci.* **6**: 139, 2015.
- Ye Z.P., Zheng Z., Kang H.J. *et al.*: [Stomatal and non-stomatal limitation characteristics of flag leaf photosynthesis in mid-maturing indica rice at early heading stage under natural conditions.] – *J. Ecol.* **38**: 1004-1012, 2019. [In Chinese]
- Zhang K., Li Y., Zhu W. *et al.*: Fine mapping and transcriptome analysis of virescent leaf gene *v-2* in cucumber (*Cucumis sativus* L.). – *Front. Plant Sci.* **11**: 570817, 2020.
- Zheng W., Shi Z., Long M. *et al.*: [Photosynthetic and physiological characteristics analysis of yellow-green leaf mutant in wheat of Jimai5265yg.] – *Sci. Agr. Sin.* **54**: 4539-4551, 2021. [In Chinese]
- Zhou H., Zhang Y., Dong W.Q. *et al.*: Heterosis effects on photosynthesis of upland cotton (*Gossypium hirsutum*) hybrid cultivars. – *Photosynthetica* **59**: 106-115, 2021.
- Zhu X., Guo S., Wang Z. *et al.*: Map-based cloning and functional analysis of *YGL8*, which controls leaf color in rice (*Oryza sativa*). – *BMC Plant Biol.* **16**: 134, 2016.